The Linnean Society of London BIOLOGICAL Journal of the Linnean Society

Biological Journal of the Linnean Society, 2015, **116**, 805–818. With 5 figures.

Diversification of body shape in *Sebastes* rockfishes of the north-east Pacific

TRAVIS INGRAM*

Department of Zoology, University of Otago, 340 Great King Street, Dunedin 9016, New Zealand

Received 2 April 2015; revised 14 June 2015; accepted for publication 14 June 2015

Body shape variation is integrally related to many aspects of fish ecology, including locomotion and foraging, and can indicate the functional diversity of fish assemblages. Few studies have thoroughly characterized body shape in a diverse marine fish clade, or investigated both temporal and spatial patterns of variation in body shape disparity. Here, I use digital photographs to measure geometric body shape in 66 species of north-east Pacific rockfish (*Sebastes* spp.), including a correction for error introduced by arching of specimens. Different components of interspecific shape variation show associations with fish size, depth habitat, trophic niche and phylogenetic relationships. Overall, the accumulation of body shape disparity appears to have been near-constant over time, and shows little variation across the latitudinal range of rockfish. © 2015 The Linnean Society of London, *Biological Journal of the Linnean Society*, 2015, **116**, 805–818.

ADDITIONAL KEYWORDS: adaptive radiation – Burnaby projection – disparity – geometric morphometrics – latitudinal diversity gradient – phylogenetic comparative methods.

INTRODUCTION

Body shape is among the most important and integrative aspects of an organism's phenotype, and advances in geometric morphometric methodology allow increasingly sophisticated study of the complex set of traits captured by shape (Adams, Rohlf & Slice, 2004). Fish are well represented in geometric morphometric studies, and associations between body shape and aspects of ecology have been documented in numerous taxonomic groups (e.g. Rüber & Adams, 2001; Clabaut *et al.*, 2007; Colombo *et al.*, 2015). Given the close relationships between shape traits and ecological function, studies of body shape can allow functional diversity to be inferred from the variety of body shapes represented in a fish community. With suitable data sets, the diversity of body shapes may thus yield clues about how functional variation arises over evolutionary time and spreads across broad spatial scales.

While some features of body shape variation are specific to taxonomic groups, there are commonalities in the major dimensions of ecologically relevant variation. In many fish clades the most important axis of body shape variation maps to benthic vs. pelagic foraging and habitat use. Pelagic fish tend to be fusiform with fins suited to sustained swimming with minimal drag, while benthic fish tend to be deeper-bodied with fins adapted to manoeuvrability and acceleration (Webb, 1984; Gerry, Robbins & Ellerby, 2012). Head and jaw traits are often related to prey capture, which can vary along the benthic–pelagic axis (e.g. feeding on benthic invertebrates vs. zooplankton) as well as with trophic position (e.g. feeding on fish vs. invertebrates; Wainwright & Richard, 1995; Aguilar-Medrano *et al.*, 2011). Adaptive variation along the benthic–pelagic axis occurs among individuals within populations (Quevedo, Svanbäck & Eklöv, 2009; Kusche *et al.*, 2014; Faulks *et al.*, 2015), between recently diverged species or ecomorphs (Schluter *et al.*, 2004; Franchini *et al.*, 2014) and across entire taxonomic groups (Claverie & Wainwright, 2014).

Most geometric morphometric studies of fish body shape have been carried out in tropical marine clades (Aguilar-Medrano *et al.*, 2011; Claverie & Wainwright, 2014), in cichlids and other diverse freshwater groups (Clabaut *et al.*, 2007; Feulner *et al.*, 2007; Sidlauskas, 2008), or in postglacial lakes with few species but high intraspecific variability

*Corresponding author. E-mail: travis.ingram@otago.ac.nz

(Schluter *et al.*, 2004; Quevedo *et al.*, 2009). Comparatively little work has been done on temperate marine fish faunas, and few studies have sought to capture the full shape diversity of an adaptively radiating group in an oceanic region (although Antarctic notothenioid fishes are a well-studied polar radiation; Colombo *et al.*, 2015). One factor limiting the breadth of studies that can be done using museum collections is arching of fish bodies due to preservation and storage, but statistical advances hold promise for making better use of existing specimens in geometric morphometric studies.

At the taxonomic and spatial scale encompassed by diverse marine fish clades, it is feasible to investigate morphological diversity (disparity) over evolutionary time and across environmental gradients. The temporal pattern of disparity accumulation can reveal large-scale macroevolutionary dynamics, such as whether disparity evolves at a steady pace over time, or if an early burst of evolution is followed by a slowdown as in classical concepts of adaptive radiation (Schluter, 2000; Harmon *et al.*, 2003, 2010). Across spatial scales, variation in disparity over latitudinal or environmental gradients may indicate how communities assemble through a combination of evolution and range shifts. Latitudinal disparity gradients might arise through variation in evolutionary rates that is associated with either environmental gradients or diversity gradients (Hipsley, Miles & Müller, 2014). The direction of any latitudinal disparity gradient will depend on whether environmental heterogeneity or species interactions are more important drivers of trait evolution, and how these drivers covary with latitude. In particular, areas with greater species diversity may either accelerate (Carlson, Wainwright & Near, 2009) or constrain (Mahler *et al.*, 2010) the evolution of further morphological disparity.

A promising group for the comparative analysis of body shape is the diverse, ecologically and economically important rockfish genus *Sebastes* (Cuvier 1829). *Sebastes* rockfish are understood to have originated in the north-west Pacific in the mid-Miocene (Hyde & Vetter, 2007) and subsequently spread throughout the north Pacific, with smaller lineages dispersing to the north Atlantic and into the Southern Hemisphere. The centre of rockfish diversity is the north-east Pacific, where at least 66 species occur between Alaska and Baja California. Diversity increases southward from 66°N to a peak at 34°N (Point Concepcion, California) where as many as 55 species occur in broad sympatry, then declines to a southern range limit at 23°N (Love, Yoklavich & Thorsteinson, 2002; Hurlbert & Stegen, 2014).

Rockfishes have been the subject of several evolutionary analyses of morphology (Ingram & Shurin, 2009; Ingram & Kai, 2014), but geometric body shape has only been investigated in two north Atlantic species (Valentin, Sévigny & Chanut, 2002; Stefánsson *et al.*, 2009; Valentin *et al.*, 2014). While rockfish do not rival the tremendous phenotypic diversity seen in freshwater clades such as cichlids (Clabaut *et al.*, 2007) and characiform fishes (Sidlauskas, 2008), they do exhibit elevated rates of diversification in species richness and ecologically relevant morphology (Rabosky *et al.*, 2013). Rockfish vary from small pelagic species such as shortbelly rockfish (*S. jordani*) to deep-bodied, robust species such as the cowcod (*S. levis*). Traits including relative eye size have been found to relate to depth habitat, while gill raker morphology is strongly correlated with diet as inferred from stable isotopes (Ingram, 2011). While rockfish fit many definitions of adaptive radiation (Schluter, 2000), morphological traits do not fit the classic pattern of an 'early burst' followed by declining evolutionary rates, rather showing considerable convergence even within the north-east Pacific (Ingram & Kai, 2014). Coupled with the group's species richness and broad latitudinal distribution, these factors make rockfish an appropriate clade in which to investigate ecological and evolutionary patterns of body shape disparity.

Here, I use geometric morphometric analyses to characterize the body shape of 66 north-east Pacific rockfish species. I obtain shape data from digital images, use a 'de-arching' procedure to remove artefacts due to specimen arching, and test for associations between body shape components and trophic morphology, habitat and body size and phylogeny. I ask whether rockfish shape evolution fits an 'early burst' pattern of temporal rate decline, but predict that shape may be more likely to show ongoing diversification as do other rockfish traits. Finally, I test whether disparity in body shape varies across the latitudinal distribution of rockfish. I hypothesize that the peak in species richness will correspond to higher or lower disparity than expected by chance, if diversity either promotes or constrains further disparity.

MATERIAL AND METHODS

Photography and landmark acquisition

I photographed rockfish specimens over a period of several years, in conjunction with morphological measurements used in other studies (Ingram & Shurin, 2009; Ingram, 2011; Ingram & Kai, 2014). In total, I photographed 110 specimens representing 65 of the 66 species in the north-east Pacific (excluding the Gulf of California) that had been described at the time data collection began (Hyde & Vetter, 2007).

Intraspecific sample sizes varied from one to four individuals (Table 1). Whenever possible I photographed sexually mature fish (above the total length of 50% maturity for that species; Froese & Pauly, 2013), but approximately 40% of specimens were subadults that fell below this threshold. Most specimens photographed (83) were from the fish collection at the Scripps Institute of Oceanography, and had been fixed in formalin and stored long-term in alcohol. These specimens were positioned vertically in a glass aquarium filled with clean water, and photographed side-on with a digital SLR camera on a tripod. A few specimens (24) were from a Department of Fisheries and Oceans Canada (DFO) trawl off the west coast of Haida Gwaii. These fish were stored frozen then thawed and photographed lying flat from above with a Nikon digital SLR camera mounted 1 m above the specimen. Three preserved specimens from the collection at the University of Washington were also photographed from above. All photographs were of the left side of the fish and included a ruler for scale. To complete the north-east Pacific data set, the species *S. rufinanus* was represented by a published photograph of the holotype (Lea & Fitch, 1972), with the scale determined by its standard length.

All analyses were carried out in the R environment (R Core Team, 2014), including geometric morphometric functions in the package 'geomorph' v. 2.1.1 (Adams & Castillo, 2013). I established the scale and digitized landmarks from each photo using the function 'digitize2d'. I selected 16 homologous landmarks on the basis of their being visible on all photos and often showing relationships with ecology in bony fishes. These landmarks capture the outline of the body and the position and relative sizes of the head, eyes and fins (Table 2, Fig. 1). All landmarks were digitized for all specimens with the exception of the one specimen of *S. borealis*, for which landmarks 1–4 were distorted (due to its mouth being stuck open) and thus coded as missing data.

Geometric morphometric analysis

I carried out a generalized Procrustes analysis (GPA) on the *Sebastes* landmark coordinates using the function 'gpagen'. This procedure consists of translating sets of coordinates to the origin, scaling them to a common size (unit 'centroid' size) and rotating them so as to maximize the alignment of coordinates among specimens. I estimated the positions of the four missing landmarks using thin-plate spline interpolation.

Error is commonly introduced into geometric morphometric studies of fishes due to the dorsoventral arching of specimens (Albert *et al.*, 2008; Valentin *et al.*, 2008). Specimens may be arched upward or downward if they are imperfectly positioned for photography, and positioning error may be impossible to avoid if specimens have been affected by formalin fixation and long-term storage. Specimen arching can manifest as a major component of shape variation with no biological meaning, such as a shape axis with low repeatability that fail to delineate groups of interest or to map to genomic locations (Albert *et al.*, 2008; Valentin *et al.*, 2008). Arching was pronounced in some specimens in the present study, and some species were not represented by any specimens that were not markedly arched. I used a statistical correction, Burnaby back-projection, to remove the arching effect from the landmark data (Burnaby, 1966; Valentin *et al.*, 2008). This technique uses a vector of coefficients that characterize the effect of arching to calculate a 'de-arched' set of adjusted landmark coordinates.

To estimate a vector describing the arching effect, I obtained five frozen red gurnard perch, *Helicolenus percoides* (Richardson & Solander, 1842), from a seafood retailer in Dunedin, New Zealand (size range: 23.6–25.8 cm total length). I used *H. percoides* due to specimen availability, but it is also appropriate due to its being a very close relative (within the subfamily Sebastinae) that is outside the focal genus, preventing the arching vector from being specific to any one species in the main analysis. Shape analyses incorporating *H. percoides* also indicate that this species occurs near the centre of the morphospace defined by *Sebastes*, and that it is thus a suitable representative for a typical rockfish shape. I photographed each thawed *H. percoides* specimen from above with a mounted Canon digital SLR camera. I took ten photographs of each fish, manually repositioning the specimen between photographs to capture the full range of dorsoventral arching of the head, body and tail. I digitized the 16 landmarks from each *H. percoides* photo, then for each of the five specimens, I carried out a GPA on the coordinates from the ten photographs. I used the geomorph function 'plotTangentSpace' to carry out a principal components analysis (PCA) on the ten sets of adjusted coordinates. For each specimen the first eigenvector explained at least 95% of the shape variation and the five first eigenvectors were aligned (mean pairwise angles between eigenvectors: $13.1 \pm 3.9°$) and clearly captured the arching effect. I used the mean of the five first eigenvectors to quantify the effect of arching on each x- and y-coordinate. I then statistically removed the arching effect from the *Sebastes* coordinates by projecting them orthogonally to the mean first eigenvector to obtain an adjusted matrix of coordinates (Burnaby, 1966; Rohlf & Bookstein, 1987; Valentin *et al.*, 2008).

Table 1. Rockfish (*Sebastes* spp.) photographed for the data set, and species mean size and shape traits from the geometric morphometric analysis

Species	*N*	Total length (cm)	log(Centroid)	PC1	PC2	PC3
aleutianus	1	26.0	3.35	−0.0399	−0.0155	0.0105
alutus	4	20.9–38.7	3.68	0.0178	−0.0058	0.0144
atrovirens	2	22.3–25.8	3.37	0.0153	0.0348	−0.0022
auriculatus	1	22.0	3.27	0.0113	0.0149	−0.0044
aurora	2	21.0–27.0	3.34	−0.0418	−0.0041	0.0130
babcocki	2	31.7–32.5	3.63	−0.0194	0.0121	−0.0195
borealis	1	54.7	4.09	−0.0102	0.0068	−0.0243
brevispinis	2	57.5–53.7	4.18	−0.0024	−0.0135	−0.0127
carnatus	1	21.3	3.24	−0.0123	0.0335	−0.0020
caurinus	2	20.8–24.1	3.28	−0.0251	0.0239	−0.0176
chlorostictus	2	22.6–23.5	3.33	−0.0241	0.0088	0.0019
chrysomelas	2	22.3–24.7	3.32	−0.0265	0.0263	−0.0222
ciliatus	1	19.8	3.15	0.0368	0.0291	0.0142
constellatus	2	16.7–18.3	3.04	−0.0256	−0.0274	−0.0019
crameri	2	24.7–23.9	3.33	−0.0360	0.0097	0.0089
dallii	1	17.2	3.06	0.0047	−0.0086	−0.0234
diploproa	1	23.4	3.24	−0.0329	−0.0204	0.0042
elongatus	4	23.5–33.1	3.47	0.0114	−0.0317	−0.0026
emphaeus	1	19.7	3.18	0.0670	−0.0094	−0.0125
ensifer	2	18.2–21.1	3.13	0.0044	−0.0150	0.0062
entomelas	1	51.6	4.13	0.0606	−0.0016	0.0060
eos	1	25.7	3.29	−0.0366	−0.0149	0.0173
flavidus	3	25.1–54.1	3.96	0.0414	0.0022	−0.0101
gilli	2	36.8–49.8	3.99	−0.0046	−0.0286	−0.0481
goodei	2	19.0–19.5	3.11	0.0534	−0.0244	0.0093
helvomaculatus	4	30.1–32.3	3.55	−0.0152	−0.0126	−0.0062
hopkinsi	2	19.9–21.2	3.22	0.0316	0.0148	0.0133
jordani	1	21.9	3.23	0.0673	−0.0327	0.0182
lentiginosus	2	20.4–22.3	3.21	−0.0226	−0.0062	−0.0021
levis	2	22.2–23.3	3.29	−0.0289	0.0007	−0.0305
macdonaldi	2	21.2–29.1	3.36	−0.0199	−0.0194	−0.0050
maliger	1	19.1	3.12	−0.0407	0.0290	0.0145
melanops	1	24.0	3.34	0.0234	0.0110	−0.0219
melanosema	1	25.7	3.42	−0.0447	−0.0209	−0.0197
melanostictus	2	25.1–57.5	3.90	−0.0147	−0.0250	−0.0041
melanostomus	2	22.8–26.7	3.35	−0.0352	−0.0200	0.0184
miniatus	2	18.6–25.2	3.25	−0.0124	0.0170	0.0058
moseri	1	19.4	3.13	0.0467	−0.0150	0.0000
mystinus	1	20.4	3.21	0.0473	0.0529	−0.0123
nebulosus	1	27.3	3.52	−0.0064	0.0192	−0.0220
nigrocinctus	2	18.3–21.1	3.16	−0.0134	0.0054	−0.0045
notius	1	22.1	3.24	−0.0534	−0.0215	0.0256
ovalis	1	26.7	3.46	0.0224	0.0213	0.0245
paucispinis	1	25.2	3.33	0.0465	−0.0373	−0.0302
phillipsi	1	37.8	3.77	−0.0380	−0.0192	−0.0055
pinniger	1	19.1	3.10	−0.0177	0.0347	0.0184
polyspinis	1	25.6	3.40	0.0282	0.0082	0.0027
proriger	3	23.8–41.8	3.75	0.0357	0.0011	0.0081
rastrelliger	2	22.8–24.1	3.36	0.0092	0.0064	−0.0231
reedi	2	39.6–47.4	3.95	0.0161	−0.0101	−0.0054
rosaceus	2	19.8–23.5	3.22	−0.0323	0.0017	−0.0060
rosenblatti	2	23.2–25.6	3.36	−0.0162	0.0000	0.0001

Table 1. *Continued*

Species	*N*	Total length (cm)	log(Centroid)	PC1	PC2	PC3
ruberrimus	2	22.8–24.4	3.32	−0.0382	0.0105	0.0080
rubrivinctus	2	29.8–31.3	3.59	−0.0356	0.0180	0.0032
rufinanus	1	16.6	3.01	0.0594	−0.0086	−0.0313
rufus	1	19.8	3.14	0.0042	−0.0096	0.0409
saxicola	1	23.6	3.32	−0.0120	0.0018	0.0255
semicinctus	2	18.2–18.5	3.07	0.0302	−0.0113	0.0281
serranoides	2	22.2–28.1	3.38	0.0395	0.0099	0.0265
serriceps	1	19.3	3.14	−0.0255	0.0351	−0.0050
simulator	1	18.3	3.08	−0.0281	−0.0194	0.0175
umbrosus	1	22.2	3.09	−0.0303	−0.0069	−0.0164
variabilis	2	31.9–32.7	3.67	0.0342	0.0170	−0.0125
variegatus	1	24.5	3.37	0.0294	0.0047	0.0240
wilsoni	1	14.4	2.84	0.0177	−0.0086	0.0341
zacentrus	4	27.0–31.4	3.51	0.0058	0.0023	0.0039

Table 2. Landmarks used to digitize rockfish shape

Landmark	Description
1	Anterior extent of maxilla
2	Anterior extent of orbit
3	Ventral extent of orbit
4	Posterior extent of orbit
5	Posterior extent of operculum
6	Anterior insertion of first dorsal spine
7	Anterior insertion of first soft dorsal fin ray
8	Posterior insertion of dorsal fin
9	Dorsal insertion of caudal fin
10	Posterior extent of lateral line
11	Ventral insertion of caudal fin
12	Posterior insertion of anal fin
13	Anterior insertion of anal spine
14	Anterior insertion of pelvic spine
15	Ventral insertion of pectoral fin
16	Dorsal insertion of pectoral fin

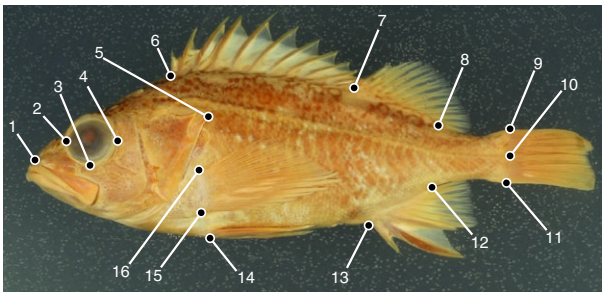

Figure 1. Position of the 16 landmarks on a rockfish specimen (*Sebastes lentiginosus*).

Using the adjusted set of coordinates, I calculated an average set of landmark coordinates for each of the 66 species. For species with multiple specimens I averaged each *x*- and *y*-coordinate, also calculating the species' average centroid size. I then carried out a PCA on the species mean, adjusted landmark data using 'plotTangentSpace'.

Associations with phylogeny, body size and ecological niche

As a phylogenetic tree, I used the maximum clade credibility tree from a recent BEAST (Drummond *et al.*, 2012) analysis of seven mitochondrial and two nuclear genes for 108 *Sebastes* species (almost the full present-day diversity of the genus) and four outgroups (Ingram & Kai, 2014). I pruned this tree to remove outgroups and *Sebastes* species from outside the north-east Pacific, thus matching the set of 66 species in the shape data set. I retained a sample of 100 trees from the posterior distribution of the BEAST analysis to assess sensitivity of results to phylogenetic uncertainty.

I compared the shape data to fish size and to two measures of the ecological niche of rockfish species. Isometric effects of size on shape are removed by the GPA procedure, but if shape changes allometrically there may still be relationships between size and shape in the resulting data set. In this data set, allometry may include both evolutionary (interspecific) allometry resulting from correlated evolution between size and shape, and ontogenetic (intraspecific) allometry due to sampling of larger or smaller individuals from different species. Ocean depth is an important environmental gradient in marine systems that shows marked variation among rockfish species. Adult rockfish occupy characteristic depth habitats ranging from subtidal to hundreds of metres deep

(Love *et al.*, 2002), and shifts in habitat depth are thought to be involved in many rockfish speciation events (Hyde *et al.*, 2008; Ingram, 2011). Dietary niche, including trophic position, differentiates many species that co-occur locally. High trophic position is strongly and negatively correlated with the length and number of gill rakers, and shows a weaker positive association with body size (Ingram & Shurin, 2009; Ingram, 2011). I used gill raker number as a morphological proxy for trophic niche as it does not change during ontogeny and as data were available for all 66 species (Ingram, 2011).

I fit phylogenetic multiple regression models to predict shape as a function of body size (log-transformed centroid size), habitat depth (square root-transformed average adult depth) and trophic niche (average gill raker number). This order of predictor variables first accounts for size-related variation, then regional-scale ecological variation (depth), then variation in local, trophic niche (different ordering has little qualitative effect on the results). I first used the geomorph function 'procD.pgls' to test whether multivariate shape was significantly related to size, depth or gill raker number. This function uses a distance-based modification of standard phylogenetic generalized least squares models to allow fitting of phylogenetically correct models when the response variable is high-dimensional. The model assumes that trait evolution follows a multivariate undirected Brownian motion (BM) random walk. To assess the validity of this assumption, I also estimated the extent of phylogenetic signal in the multidimensional shape data using K_{mult}, a modification of Blomberg's K statistic (Blomberg, Garland & Ives, 2003; Adams, 2014). This statistic indicates whether shape variation is as structured by phylogeny as expected under BM ($K_{\text{mult}} = 1$) or shows higher ($K_{\text{mult}} > 1$) or lower ($K_{\text{mult}} < 1$) phylogenetic signal. I used 999 permutations to test for significant phylogenetic signal (i.e. $K_{\text{mult}} > 0$), and repeated the calculations for each of the 100 trees.

The distance-based version of PGLS is currently limited by an inability to consider non-Browian evolution, which may reduce phylogenetic signal. It also does not allow consideration of whether particular dimensions of shape variation are related to different organismal or ecological characteristics. Thus, I also fit univariate PGLS models to the first three PC shape axes, while simultaneously estimating another measure of phylogenetic signal in each axis, Pagel's λ (Pagel, 1999; Freckleton, Harvey & Pagel, 2002). This scaling parameter transforms the internal branch lengths of the phylogeny to reflect strong phylogenetic signal ($\lambda = 1$, consistent with BM), no phylogenetic signal ($\lambda = 0$) or intermediate signal ($0 < \lambda < 1$). I fit univariate models to each shape PC axis with the same three predictor variables using the R function 'pgls' in the package 'caper'. I also used likelihood ratio tests to compare the model with estimated λ to a model with no phylogenetic signal ($\lambda = 0$) to test for the presence of phylogenetic signal in each PC axis. To facilitate interpretation of regression coefficients, I first centred and scaled all response and predictor variables to unit standard deviation. Again, I repeated this analysis for all 100 trees.

Disparity accumulation over time and space

I visualized the evolutionary history of rockfish shape using a 'phylomorphospace', which projects the branches of a phylogenetic tree into a two-dimensional morphospace defining trait variation among species (Sidlauskas, 2008). If subclades occupy large regions of this morphospace the implication is that recent divergence contributes substantially to overall morphological diversity or 'disparity', while if subclades occupy limited morphospace the implication is that most disparity is accounted for by earlier divergence, consistent with an early burst of trait evolution. I generated phylomorphospace plots for PC1 and PC2, and for PC1 and PC3, using the 'phylomorphospace' function in the R package 'phytools' (Revell, 2012). I coloured edges and nodes of the projected tree to indicate several named or notable subclades within *Sebastes*, largely consistent with Hyde & Vetter (2007) and all receiving strong support in the BEAST analysis (each subclade had a posterior probability of 1.0; Ingram & Kai, 2014).

I then investigated how rockfish shape disparity has accumulated over the group's evolutionary history. Disparity is a multivariate extension of the variance, and for high-dimensional data can be calculated using distances as a Procrustes variance (Zelditch, Swiderski & Sheets, 2012). I visualized the timing of disparity accumulation by using a disparity-through-time (DTT) plot to graph the relative contribution of subclades to overall disparity as the clade diversifies (Harmon *et al.*, 2003; Colombo *et al.*, 2015). If the rate of morphological diversification is constant, as expected under BM, this DTT curve will decrease linearly toward zero through the clade's evolutionary history. Under an 'early burst' model, the within-subclade disparity will decline much earlier, while if morphospace is constrained or if evolution within subclades is fast, the observed DTT curve may fall above the Brownian expectation. I obtained the morphological disparity index (MDI) statistic, measured as the area between the observed DTT curve and the median of 999 simulated DTT curves (Harmon *et al.*, 2003), using the R package geiger (Harmon *et al.*, 2008). I tested for significance by

comparing the MDI with the null distribution, asking whether the DTT curve fell above (positive MDI) or below (negative MDI) the BM expectation, and repeated this for each of the 100 trees.

Finally, I asked how disparity varies across the latitudinal gradient of the north-east Pacific. I used published latitudinal ranges (Love *et al.*, 2002; Froese & Pauly, 2013) to represent the distribution of each species along the west coast of North America. I identified the set of species whose ranges overlap with each degree latitude, and calculated diversity as the number of species present at that latitude (these species may or may not coexist at small scales depending on their depth habitat). I restricted latitudes to the range 25–65°N, to include only latitudinal bands with species richness > 5 and thus avoid effects of very small sample sizes. I then calculated the Procrustes disparity of the set of species present at each latitude, and scaled each measure to the maximum disparity at any latitude.

To test whether the trend of disparity across latitudes deviates from a null expectation, I used a similar approach to the DTT analysis. This is necessary because adjacent latitudes share species and are thus non-independent. I simulated 999 morphological data sets under multivariate BM, then, preserving species identities and latitudinal distributions, recalculated the relative disparity at each latitude for each simulated data set. I displayed the observed and expected curves for 'disparity-through-space' in a manner analogous to DTT plots, with the observed trend in relative disparity compared with median and 95% ranges across the simulations. I calculated a metric analogous to the MDI statistic (here called $MDI_{latitude}$) based on the area between the observed and median null curves, after first scaling the length of the *x*-axis to 1 for consistency with the DTT analysis. The only difference from the MDI calculations is that I used the cumulative absolute deviation between the curves to measure the discrepancy between the observed and median null curves (MDI uses the cumulative directional discrepancy between curves). This means that while the MDI can be positive or negative, $MDI_{latitude}$ can only be positive, with its interpretation depending on how the curves differ. I thus assessed significance with a one-tailed test by comparison with values calculated for the simulated data sets, and repeated the analysis for each tree.

RESULTS

Geometric morphometric analysis

Specimen arching had a strong effect on shape variation when a PCA was run on species-averaged landmark data that had not been corrected for the arching effect. In this case PC2 mainly captured the arching artefact, with a strong correlation between the second eigenvector and the vector **f** derived from the manually arched *H. percoides* specimens ($r = 0.82$). The Burnaby back-projection effectively removed this artefact, resulting in eigenvectors entirely uncorrelated with **f** (Fig. 2).

The first three axes from the PCA of species mean adjusted landmark coordinates explained 38, 14 and 12% of shape variation. Later axes each explained < 10% of shape variation, and typically showed little if any relationship to phylogeny, body size or niche measures, so they are not considered individually in what follows. The first principal component axis describes relative head size and body depth, with large values of PC1 corresponding to smaller heads, more anterior pelvic and pectoral fins, narrower bodies and longer caudal peduncles (Fig. 3). Pelagic species such as *S. jordani*, *S. emphaeus* and *S. entomelas* had the largest PC1 values, while the benthic species *S. notius*, *S. melanosema* and *S. aurora* had the lowest. An increase in PC2 indicates deeper bodies but smaller heads, as well as smaller eyes relative to head size. Larger values of PC3 indicate relatively larger eyes, more anterior anal fins and somewhat narrower bodies.

Associations with phylogeny, body size and ecological niche

The distance-based PGLS analysing overall body shape as a function of size, depth habitat and gill raker number showed modest relationships. Body size (log-transformed centroid size) and gill raker number were both marginally significant predictors of shape (body size: $F_{1,62} = 4.4$, $P = 0.068$; gill raker number: $F_{1,62} = 2.0$, $P = 0.095$), while depth habitat was not significantly associated with overall shape ($F_{1,62} = 2.0$, $P = 0.24$). Across trees from the posterior distribution, size was significant (at $\alpha = 0.05$) for 4% of trees, vs. 0% for depth and 16% for gill raker number. The multivariate measure of phylogenetic signal was estimated as $K_{mult} = 0.35$, below the Brownian expectation of 1, but significantly greater than expected if traits were unstructured by phylogeny ($P = 0.001$). K_{mult} ranged from 0.26 to 0.41 across trees, and was consistently significantly higher than 0 (all $P < 0.01$).

PGLS analyses of individual PC axes revealed relationships between ecological traits and specific dimensions of shape variation (Table 3). PC1 was positively related to gill raker number, indicating that, as expected, species with more pelagic body shapes tend to feed on lower trophic level prey such as zooplankton. PC2 was strongly and negatively related to depth habitat, indicating that deeper-bodied

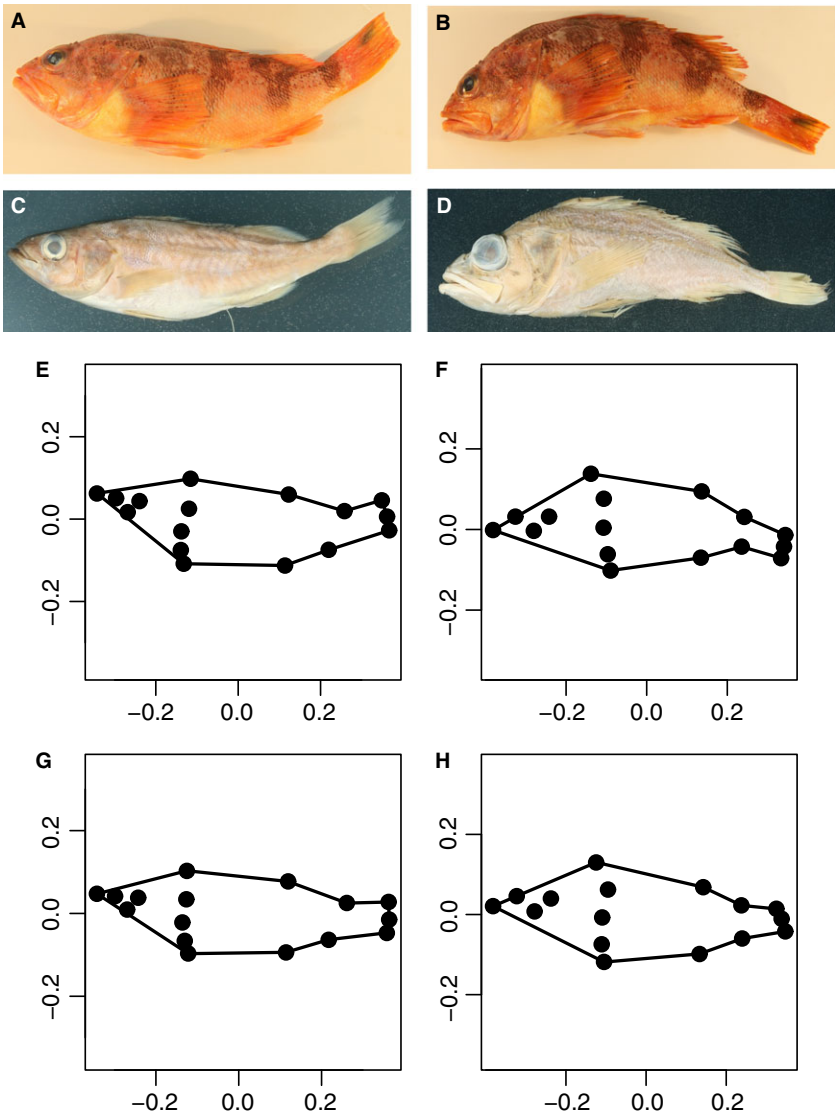

Figure 2. Demonstration of the 'de-arching' protocol applied to *Sebastes* landmark data. A, B, a single specimen of *Helicolenus percoides* photographed with different degrees of arching. C, D, the most upwardly arched specimen (*S. goodei*) and the most downwardly arched specimen (*S. melanostictus*). E, F, landmark positions for the specimens in C and D prior to de-arching. G, H, adjusted landmark positions after applying Burnaby's back projection to statistically remove the effect of arching.

species with relatively smaller heads and eyes are found in shallower depth strata. PC3 showed a negative relationship with log-transformed centroid size, as well as a positive relationship with gill raker number. PC1 and PC2 had relatively high phylogenetic signal, with estimated λ values of 0.83 and 0.85, respectively, both significantly greater than zero. PC3 was estimated to show no phylogenetic signal ($\lambda = 0$). This is reflected in the phylomorphospace figures (Fig. 4), where species within subclades tend to be clustered for PC1 and PC2, but not for PC3. PGLS results were qualitatively identical across the 100 trees, with the same predictor variables consistently significant for each analysis.

Disparity accumulation over time and space

The DTT analysis revealed that body shape disparity tends to be partitioned within rather than between subclades, although not significantly more than expected under BM (Fig. 5A; MDI = 0.274, $P = 0.12$). The observed DTT curve fell within the range of the expectation under BM for the first half of the evolutionary history of *Sebastes*, while

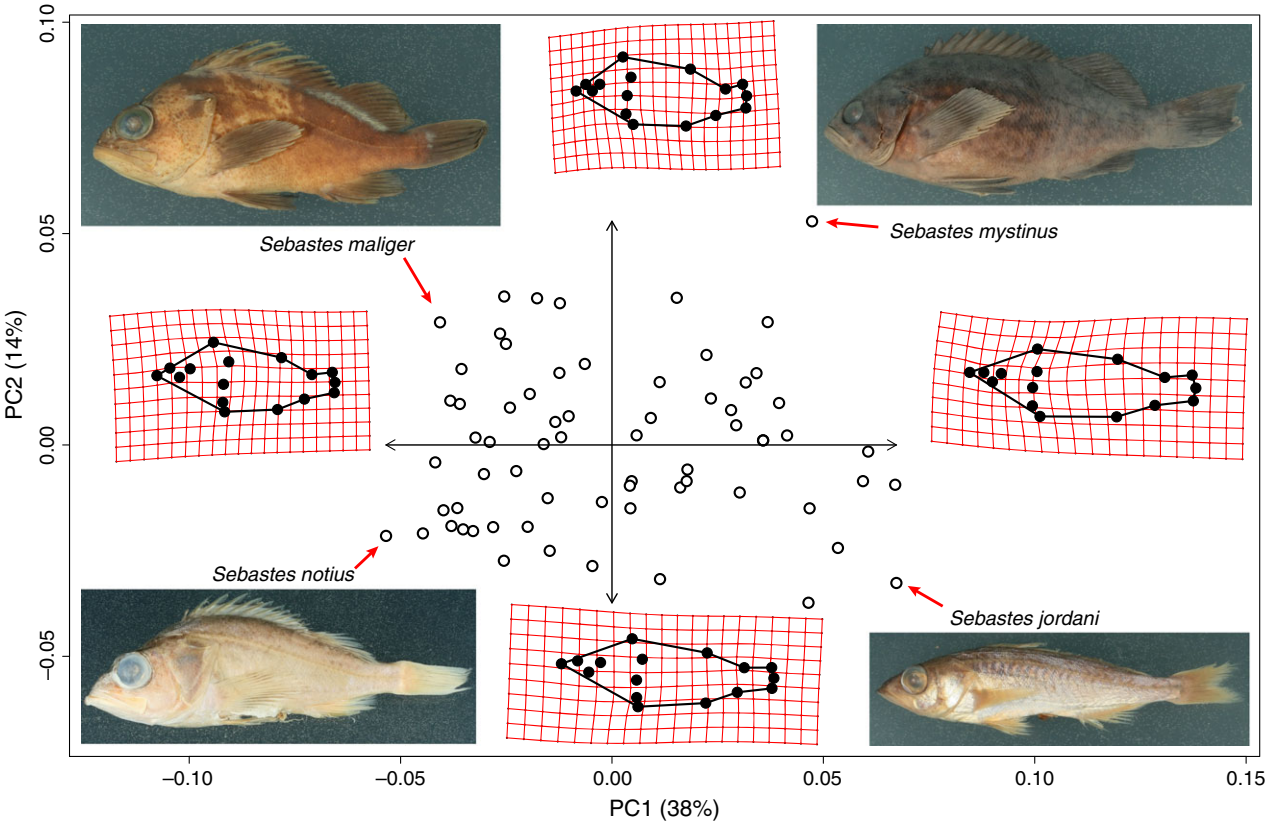

Figure 3. Shape variation among *Sebastes* species. Deformation grids show the shape change associated with the first two principal component axes PC1 and PC2, and photos display selected species in each quadrant of this two-dimensional shape space.

Table 3. Results of phylogenetic generalized least squares analysis predicting each of the first three PC shape axes from body size, depth habitat and gill raker number

	Body size			Depth habitat			Gill raker number			Phylogenetic signal	
	β	SE	*P*	β	SE	*P*	β	SE	*P*	λ	*P* (λ > 0)
PC1	0.119	0.099	0.23	−0.196	0.131	0.14	**0.298**	**0.106**	**0.007**	**0.83**	**0.00003**
PC2	−0.036	0.101	0.73	**−0.480**	**0.136**	**0.0008**	−0.107	0.109	0.33	**0.85**	**0.0096**
PC3	**−0.375**	**0.120**	**0.0028**	0.208	0.123	0.094	**0.276**	**0.114**	**0.018**	0.00	1

For phylogenetic signal λ, the *P*-value comes from a likelihood ratio test against the null hypothesis of no phylogenetic signal (λ = 0). Boldface indicates significant relationships ($P < 0.05$).

over the past 4 Myr subclades contained a greater proportion of the total disparity than expected under BM. At no point did the observed DTT curve fall below the Brownian expectation as predicted if disparity evolved in an early burst. Across the 100 trees, the MDI ranged from 0.256 to 0.303, and was significantly greater than zero only once.

Disparity over space also largely followed the expectation under BM. Whereas species richness peaks sharply at a latitude of 34°N, relative disparity has a broad, flat peak with a maximum in the middle of the range, between approximately 40 and 50°N (Fig. 5B). The observed disparity across latitudes was very similar to the median of the data sets simulated under BM. The $MDI_{latitude}$ of 0.036 (range

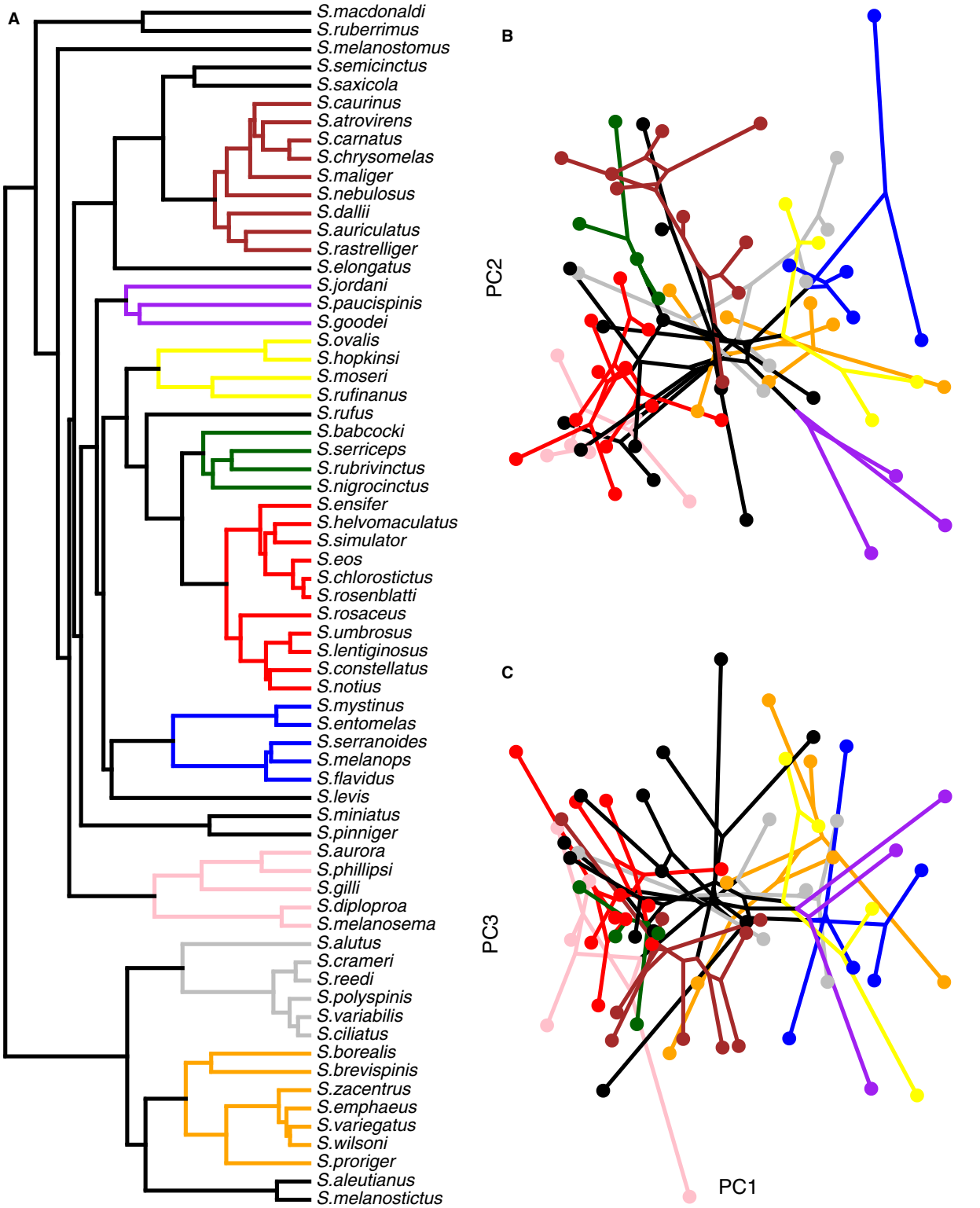

Figure 4. A, phylogenetic tree for 66 species of north-east Pacific rockfish. Notable subclades are highlighted in colour: *Pteropodus* (brown), *Sebastodes* (purple), *Acutomentum* (yellow), *Sebastichthyes* (green); *Sebastomus* (red), *Sebastosomus* (blue), *Eosebastes* (pink), *Sebastes* (grey) and Clades A + B from Hyde and Vetter (2007) (orange). B, phylomorphospace plot projecting the tree into PC shape space (PC1 and PC2), with ancestral characters estimated using maximum likelihood and subclades coloured to match the tree. C, phylomorphospace for PC1 and PC3.

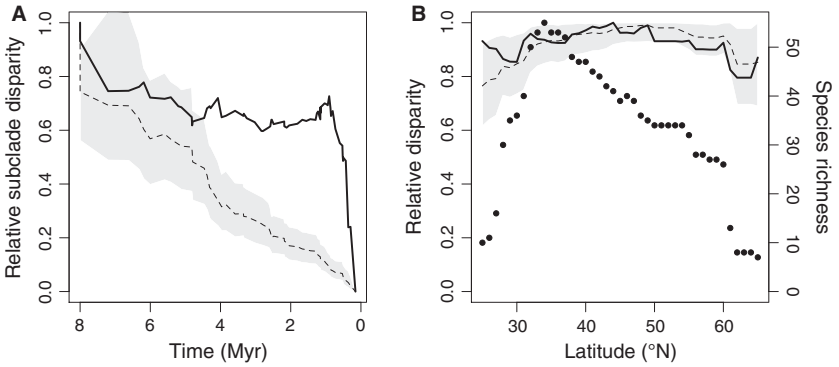

Figure 5. A, disparity-through-time estimated for rockfish shape. The solid line indicates the relative subclade disparity across the evolutionary history of *Sebastes*. The dashed line and the grey shading indicate the median and 95% range of disparity across 999 simulations under Brownian motion. B, diversity and disparity gradients with latitude. Filled circles indicate the species richness at each latitude. Disparity is displayed as in (A), with the observed pattern of disparity (relative to the maximum) at each latitude indicated with the solid line, and the median and 95% range of simulated values indicated with the dashed line and grey shading.

across trees 0.027–0.057) was not significantly greater than zero (one-tailed $P = 0.27$; non-significant for all 100 trees).

DISCUSSION

Body shape in *Sebastes* rockfishes shows associations with ecological niche axes, with the dominant component of shape variation corresponding largely to the benthic–pelagic axis and secondary axes related to depth habitat and allometry. Patterns of disparity through evolutionary time and across the latitudinal range of *Sebastes* generally follow the predictions of a simple model of constant and undirected shape diversification.

The shape data analysed here should be considered in light of several limitations to the sampling design and methodology. Because photographs were taken opportunistically at multiple locations, it was not possible to standardize the conditions, aside from ensuring that photographs were as close to side-on as possible with all landmark traits visible. Furthermore, the very small sample sizes for each species (usually one specimen, and at most four) obviously limits the precision with which species mean shapes can be characterized. Error in estimates of species means can result from true intraspecific shape variation, including allometric variation and sexual dimorphism, in addition to measurement error associated with the preservation and positioning of specimens. While as many specimens as possible were reproductive-sized adults, the long post-maturity growth period of rockfish means that there is no 'typical' body size of species, and requires a large sample to fully account for allometry. Intraspecific allometry in some morphometric traits has been found in adult rockfish: some traits are more likely to exhibit negative allometry (e.g. eye size), while others exhibit isometry (e.g. caudal peduncle length) or positive allometry (e.g. body depth; Chen, 1971). Rockfish are not visibly sexually dimorphic, although subtle dimorphism in some metric traits has been reported in a few species (Chen, 1971; Echeverria, 1986). Unfortunately, with limited intraspecific sampling it is impossible to isolate these sources of variation in the present data set. While high intraspecific variation or measurement error obscures phylogenetic signal, the error in estimating species means was clearly not sufficient to mask the presence of relatively strong signal in at least the first two shape PC axes.

In this study, as in many photographic studies of fish shape, dorsoventral arching of the body had a considerable and specific effect on the placement of landmarks. In the absence of data on how this arching affects landmark positions it can be challenging to separate from variation in body form, but the Burnaby back-projection approach employed here provides a solution (Valentin *et al.*, 2008). By transforming the landmark data to force it to be orthogonal to a vector defining arching in known specimens (in this case *H. percoides*), this approach removes most of the signal of arching in the specimens of interest. There is of course no guarantee that arching affects all specimens equally, and species in a comparative sample may differ in how arching affects landmark positions. The use of a close relative with a similar shape but outside the focal genus sidesteps the issue of whether the arching vector applies to only particular species in the data set, but ideally the arching vector would be compared between numerous species in the focal

clade. This is challenging when sampling all species requires the use of preserved museum specimens. While fresh samples and uniform techniques for positioning and photographing specimens are ideal, this study shows how properly applied statistical procedures can be used to extract meaningful data from poorly positioned specimens in comparative samples.

Shape variation in rockfish encompasses a range of characteristics, although relative body elongation (length relative to body depth) is an important contributor to the first PC axis, which explained 38% of the total variation. This is consistent with results from Claverie & Wainwright (2014), who found that in most reef fish families, shape PC1 is significantly aligned with relative elongation. They found this relationship to be significant for the Scorpaenidae (including *Sebastes*), although the alignment was weaker than in many families. Accordingly, in the present study PC1 was not exclusively related to relative elongation, and incorporated variation in fin and head dimensions. Thus, while relative elongation is involved in *Sebastes* shape variation, as it is across numerous extant and extinct fishes (Friedman, 2010; Claverie & Wainwright, 2014), it is only a part of the story of rockfish disparity.

The ecological associations with body shape identified here are consistent with established relationships between morphology and ecology in *Sebastes*. In particular PC1 was strongly associated with gill raker number, a proxy for species' trophic niches, while PC2 was strongly associated with depth habitat. Taken together, these relationships support previous indications that rockfish species can be characterized by their positions along a critical macrohabitat niche axis (depth), and by their use of dietary resources, captured in part by trophic position (Ingram & Shurin, 2009; Ingram, 2011). Divergence in adult depth habitat, with accompanying variation in body shape and eye size, appears to be involved in many speciation events in rockfish (Hyde *et al.*, 2008; Ingram, 2011), and may help to explain their high diversity at broad-scale sympatry (i.e. at the same latitude). Past studies have focused on gill rakers as a key morphological correlate of diet (Ingram & Shurin, 2009; Ingram, 2011; Ingram & Kai, 2014). The observed strong association between gill rakers and PC1 indicate that they are a part of a more integrative trait complex that relates to foraging and prey capture by rockfish. While rockfish ecology certainly incorporates other features such as microhabitat variation (e.g. use of hard vs. soft substrate), temporal activity and use of specific prey items, these results support the view that much of the ecomorphological diversity of rockfish is associated with two key niche axes.

The DTT analysis reveals how body shape disparity has evolved over the course of the evolutionary history of *Sebastes*. Early in the clade's evolution, disparity accumulates steadily as the major subclades gradually become distinct from one another. Modern subclades do tend to occupy distinct regions of morphospace, at least in the first two dimensions of shape variation (Fig. 4B). However, the observed within-subclade disparity does become substantially elevated over the Brownian expectation later on (Fig. 5A), probably reflecting the influence of shape variation (including PC3) that shows little signal of phylogeny. Species means on these minor axes (PC3 and higher) are likely to be influenced by intraspecific variation or measurement error, inflating the within-subclade disparity. While the MDI did not depart from a null expectation even in the full analysis, it becomes much smaller (indicating a closer fit to BM) if the DTT analysis is repeated with only the first two PC axes (MDI = 0.04 instead of 0.27). Thus, there is no overall indication that the evolution of shape diversity in rockfish departs from the expectation under a constant evolutionary rate, adding to the number of cases showing no evidence of early bursts of shape disparity evolution (Harmon *et al.*, 2003, 2010; Ingram, Harmon & Shurin, 2012).

This study applied the DTT methodology in a novel context to examine how relative disparity varies across a latitudinal gradient in rockfish. While latitudinal richness gradients are extremely well studied, latitudinal trends in disparity are rarely investigated (but see Hipsley *et al.*, 2014). A latitudinal disparity gradient could exist because species diversity either promotes or constrains further morphological evolution, because environmental heterogeneity varies along the gradient, or because of how species historically spread across latitudes. In rockfish, the spread through the north-east Pacific was north-to-south (Hyde & Vetter, 2007), but the southern peak in species richness implies that historical spread does not constrain present diversity. Still, this history could have resulted in a disparity gradient if distinct subclades remained restricted to ancestral (northern) waters or only formed after migrating south. Instead, I found that disparity was very near constant across the latitudinal range of *Sebastes*, with a shallow peak at mid-latitudes that is almost perfectly predicted by a combination of Brownian evolution and the observed latitudinal distribution of rockfish lineages (Fig. 5B). The variability of species in shape space thus does not seem to depend on ecological or historical factors associated with this broad latitudinal gradient.

This study continues the characterization of an important radiation of temperate marine fish. While rockfish do not exhibit an early burst of phenotypic diversification early in their history, they can

nonetheless be considered an adaptive radiation due to their rapid speciation rate, trait–environment relationships and divergence along ecological niche axes (Schluter, 2000). To the extent that body shape reflects ecological function, this study suggests that the functional diversity of rockfish assemblages has arisen steadily over time and is relatively constant across broad spatial scales.

ACKNOWLEDGEMENTS

I thank K. Maslenikov, H. J. Walker and K. L. Yamanaka for access to rockfish specimens, and O. L. Lau, K. Miller and H. J. Walker for assistance with photography. The manuscript was improved by comments from three anonymous referees. The research underlying this manuscript was supported in part by the National Science and Engineering Research Council of Canada (NSERC).

REFERENCES

Adams DC. 2014. A generalized K statistic for estimating phylogenetic signal from shape and other high-dimensional multivariate data. *Systematic Biology* **63:** 685–697.

Adams DC, Castillo EO. 2013. geomorph: an R package for the collection and analysis of geometric morphometric shape data. *Methods in Ecology and Evolution* **4:** 393–399.

Adams DC, Rohlf FJ, Slice DE. 2004. Geometric morphometrics: ten years of progress following the 'revolution'. *Italian Journal of Zoology* **71:** 5–16.

Aguilar-Medrano R, Frédérich B, de Luna E, Balart EF. 2011. Patterns of morphological evolution of the cephalic region in damselfishes (Perciformes: Pomacentridae) of the Eastern Pacific. *Biological Journal of the Linnean Society* **102:** 593–613.

Albert AYK, Sawaya S, Vines T, Knecht AK, Miller CT, Summers BR, Balabhadra S, Kingsley DM, Schluter D. 2008. The genetics of adaptive shape shift in stickleback: pleiotropy and effect size. *Evolution* **62:** 76–85.

Blomberg SP, Garland T Jr, Ives AR. 2003. Testing for phylogenetic signal in comparative data: behavioral traits are more labile. *Evolution* **57:** 717–745.

Burnaby TP. 1966. Growth-invariant discriminant functions and generalized distances. *Biometrics* **22:** 96–110.

Carlson RL, Wainwright PC, Near TJ. 2009. Relationship between species co-occurrence and rate of morphological change in *Percina* darters (Percidae: Etheostomatinae). *Evolution* **63:**767–778.

Chen LC. 1971. Systematics, variation, distribution, and biology of rockfishes of the subgenus *Sebastomus* (Pisces, Scorpaenidae, *Sebastes*). *Bulletin of the Scripps Institution of Oceanography, UC San Diego* **18:** 1–115.

Clabaut C, Bunje PME, Salzburger W, Meyer A. 2007. Geometric morphometric analyses provide evidence for the adaptive character of the Tanganyikan cichlid fish radiations. *Evolution* **61:** 560–578.

Claverie T, Wainwright PC. 2014. A morphospace for reef fishes: elongation is the dominant axis of body shape evolution. *PLoS ONE* **9:** e112732.

Colombo M, Damerau M, Hanel R, Salzburger W, Matschiner M. 2015. Diversity and disparity through time in the adaptive radiation of Antarctic notothenioid fishes. *Journal of Evolutionary Biology* **28:** 376–394.

Drummond AJ, Suchard MA, Xie D, Rambaut A. 2012. Bayesian phylogenetics with BEAUti and the BEAST 1.7. *Molecular Biology and Evolution* **29:** 1969–1973.

Echeverria TW. 1986. Sexual dimorphism in four species of rockfish genus *Sebastes* (Scorpaenidae). *Environmental Biology of Fishes* **15:** 181–190.

Faulks L, Svanbäck R, Eklöv P, Östman Ö. 2015. Genetic and morphological divergence along the littoral–pelagic axis in two common and sympatric fishes: perch, *Perca fluviatilis* (Percidae) and roach, *Rutilus rutilus* (Cyprinidae. *Biological Journal of the Linnean Society* **114:** 929–940.

Feulner PGD, Kirschbaum F, Mamonekene V, Ketmaier V, Tiedemann R. 2007. Adaptive radiation in African weakly electric fish (Teleostei: Mormyridae: *Campylomormyrus*): a combined molecular and morphological approach. *Journal of Evolutionary Biology* **20:** 403–414.

Franchini P, Fruciano C, Spreitzer ML, Jones JC, Elmer KR, Henning F, Meyer A. 2014. Genomic architecture of ecologically divergent body shape in a pair of sympatric Crater Lake cichlid fishes. *Molecular Ecology* **23:** 1828–1845.

Freckleton R, Harvey P, Pagel M. 2002. Phylogenetic analysis and comparative data: a test and review of evidence. *American Naturalist* **160:** 712–726.

Friedman M. 2010. Explosive morphological diversification of spiny-finned teleost fishes in the aftermath of the end-Cretaceous extinction. *Proceedings of the Royal Society B: Biological Sciences* **277:** 1675–1683.

Froese R, Pauly D. 2013. *FishBase*. World Wide Web electronic publication, version (04/2013). Available at: www.-fishbase.org

Gerry SP, Robbins A, Ellerby DJ. 2012. Variation in fast-start performance within a population of polyphenic bluegill (*Lepomis macrochirus*). *Physiological and Biochemical Zoology* **85:** 694–703.

Harmon LJ, Schulte JA, Larson A, Losos JB. 2003. Tempo and mode of evolutionary radiation in iguanian lizards. *Science* **301:** 961–964.

Harmon LJ, Weir JT, Brock CD, Glor RE, Challenger W. 2008. GEIGER: investigating evolutionary radiations. *Bioinformatics* **24:** 129–131.

Harmon LJ, Losos JB, Davies TJ, Gillespie RG, Gittleman JL, Jennings WB, Kozak KH, McPeek MA, Moreno-Roark F, Near TJ, Purvis A, Ricklefs RE, Schluter D, Schulte II JA, Seehausen O, Sidlauskas BL, Torres-Carvajal O, Weir JT, Mooers AØ. 2010. Early bursts of body size and shape evolution are rare in comparative data. *Evolution* **64:** 2385–2396.

Hipsley CA, Miles DB, Müller J. 2014. Morphological disparity opposes latitudinal diversity gradient in lacertid lizards. *Biology Letters* **10:** 20140101.

Hurlbert AH, Stegen JC. 2014. When should species richness be energy limited, and how would we know? *Ecology Letters* **17:** 401–413.

Hyde JR, Vetter RD. 2007. The origin, evolution, and diversification of rockfishes of the genus *Sebastes* (Cuvier). *Molecular Phylogenetics and Evolution* **44:** 790–811.

Hyde JR, Kimbrell CA, Budrick JE, Lynn EA, Vetter RD. 2008. Cryptic speciation in the vermilion rockfish (*Sebastes miniatus*) and the role of bathymetry in the speciation process. *Molecular Ecology* **17:** 1122–1136.

Ingram T. 2011. Speciation along a depth gradient in a marine adaptive radiation. *Proceedings of the Royal Society B: Biological Sciences* **278:** 613–618.

Ingram T, Kai Y. 2014. The geography of morphological convergence in the radiations of Pacific *Sebastes* rockfishes. *American Naturalist* **184:** E115–E131.

Ingram T, Shurin JB. 2009. Trait-based assembly and phylogenetic structure in northeast Pacific rockfish assemblages. *Ecology* **90:** 2444–2453.

Ingram T, Harmon LJ, Shurin JB. 2012. When should we expect early bursts of trait evolution in comparative data? Predictions from an evolutionary food web model. *Journal of Evolutionary Biology* **25:** 1902–1910.

Kusche H, Recknagel H, Elmer KR, Meyer A. 2014. Crater Lake cichlids individually specialize along the benthic–limnetic axis. *Ecology and Evolution* **4:** 1127–1139.

Lea RN, Fitch JE. 1972. *Sebastes rufinanus*, a new scorpaenid fish from Californian waters. *Copeia* **1972:** 423–427.

Love MS, Yoklavich M, Thorsteinson LK. 2002. *The rockfishes of the northeast Pacific*. Berkeley, CA: University of California Press.

Mahler DL, Revell LJ, Glor RE, Losos JB. 2010. Ecological opportunity and the rate of morphological evolution in the diversification of Greater Antillean anoles. *Evolution* **64:** 2731–2745.

Pagel M. 1999. Inferring the historical patterns of biological evolution. *Nature* **401:** 877–884.

Quevedo M, Svanbäck R, Eklöv P. 2009. Intrapopulation niche partitioning in a generalist predator limits food web connectivity. *Ecology* **90:** 2263–2274.

R Core Team. 2014. *R: a language and environment for statistical computing*. Vienna: R Foundation for Statistical Computing.

Rabosky DL, Santini F, Eastman J, Smith SA, Sidlauskas B, Chang J, Alfaro ME. 2013. Rates of speciation and morphological evolution are correlated across the largest vertebrate radiation. *Nature Communications* **4:** 1–8.

Revell LJ. 2012. Phytools: an R package for phylogenetic comparative biology (and other things). *Methods in Ecology and Evolution* **3:** 217–223.

Rohlf FJ, Bookstein FL. 1987. A comment on shearing as a method for 'size correction'. *Systematic Biology* **36:** 356–367.

Rüber L, Adams DC. 2001. Evolutionary convergence of body shape and trophic morphology in cichlids from Lake Tanganyika. *Journal of Evolutionary Biology* **14:** 325–332.

Schluter D. 2000. *The ecology of adaptive radiation*. Oxford, UK: Oxford University Press.

Schluter D, Clifford EA, Nemethy M, McKinnon JS. 2004. Parallel evolution and inheritance of quantitative traits. *American Naturalist* **163:** 809–822.

Sidlauskas B. 2008. Continuous and arrested morphological diversification in sister clades of characiform fishes: a phylomorphospace approach. *Evolution* **62:** 3135–3156.

Stefánsson MÖ, Sigurdsson T, Pampoulie C, Daníelsdóttir AK, Thorgilsson B, Ragnarsdóttir A, Gíslason D, Coughlan J, Cross TF, Bernatchez L. 2009. Pleistocene genetic legacy suggests incipient species of *Sebastes mentella* in the Irminger Sea. *Heredity* **102:** 514–524.

Valentin AE, Sévigny JM, Chanut JP. 2002. Geometric morphometrics reveals body shape differences between sympatric redfish *Sebastes mentella*, *Sebastes fasciatus* and their hybrids in the Gulf of St Lawrence. *Journal of Fish Biology* **60:** 857–875.

Valentin AE, Penin X, Chanut JP, Sévigny JM, Rohlf FJ. 2008. Arching effect on fish body shape in geometric morphometric studies. *Journal of Fish Biology* **73:** 623–638.

Valentin AE, Penin X, Power D, Chanut JP, Sévigny JM. 2014. Combining microsatellites and geometric morphometrics for the study of redfish (*Sebastes* spp.) population structure in the Northwest Atlantic. *Fisheries Research* **154:** 102–119.

Wainwright PC, Richard BA. 1995. Predicting patterns of prey use from morphology of fishes. *Environmental Biology of Fishes* **44:** 97–113.

Webb PW. 1984. Body form, locomotion and foraging in aquatic vertebrates. *American Zoologist* **24:** 107–120.

Zelditch ML, Swiderski DL, Sheets HD. 2012. *Geometric morphometrics for biologists: a primer*. New York: Academic Press.